coding. In: Greitz T, Ingvar DH, Widen L, eds. *The metabolism of the human brain studied with positron emission tomography.* New York, NY: Raven Press; 1985:13–19.
28. Chesler DA. Positron tomography and three-dimensional reconstruction technique. In: Freedman GS, ed. *Tomographic imaging in nuclear medicine.* New York, NY: Society of Nuclear Medicine; 1973;374–378.
29. Laruelle M, Wallace E, Seibyl JP, et al. Graphical, kinetic and equilibrium analyses of in vivo [^{123}]β-CIT binding to dopamine transporters in healthy human subjects. *J Cereb Blood Flow Metab* 1994;14:982–994.
30. Wong DF, Yung B, Dannals RF, et al. In vivo imaging of baboon and human dopamine transporters by positron emission tomography using [^{11}C]WIN 35,428. *Synapse* 1993;15:130–142.
31. Hoffman EJ, Huang S-C, Phelps ME. Quantitation in positron emission computed tomography. 1. Effect of object size. *J Comp Assist Tomogr* 1979;3:299–308.
32. Szabo J, Cowan WM. A stereotactic atlas of the brain of the cynomolgus monkey (macaca fascicularis). *J Comp Neurol* 1984;222:265–300.
33. Carroll FI, Rahman MA, Abraham P, et al. Iodine-123-3β-(4-iodophenyl)tropan-2β-carboxylic acid methyl ester (RTI-55), a unique cocaine receptor ligand for imaging the dopamine and serotonin transporters in vivo. *Med Chem Res* 1991;1:289–294.
34. Neumeyer JL, Wang S, Milius RA, et al. [^{123}I]2β-carbomethoxy-3β-(4-iodophenyl)tropane (β-CIT): high affinity SPECT radiotracer of monoamine reuptake sites in brain. *J Med Chem* 1991;34:144–146.
35. Boja JM, Mitchell WM, Patel A, et al. High-affinity binding of [^{125}I]RTI-55 to dopamine and serotonin transporters in rat brain. *Synapse* 1992;12:27–36.
36. Muller L, Halldin C, Farde L, et al. [^{11}C]β-CIT, a cocaine analogue. Preparation, autoradiography and preliminary PET investigations. *Nucl Med Biol* 1993;20:249–255.
37. Hantraye P, Brownell A-L, Elmaleh D, et al. Dopamine fiber detection by [^{11}C]-CFT and PET in a primate model of Parkinsonism. *Neuro Report* 1992;3:265–268.
38. Wullner U, Pakzaban P, Brownell A-L, et al. Dopamine terminal loss and onset of motor symptoms in MPTP-treated monkeys: a positron emission tomography study with ^{11}C-CFT. *Exp Neurol* 1994;126:305–309.
39. Frost JJ, Rosier AJ, Reich SG, et al. Positron emission tomographic imaging of the dopamine transporter with ^{11}C-WIN 35,428 reveals marked declines in mild Parkinson's disease. *Ann Neurol* 1993;34:423–431.

Age-Related Diminution of Dopamine Antagonist-Stimulated Vesamicol Receptor Binding

Simon M.N. Efange, Rosemary B. Langason and Anil B. Khare
Departments of Radiology, Medicinal Chemistry and Neurosurgery, University of Minnesota, Minneapolis, Minnesota

Previous studies of radiolabeled vesamicol receptor (VR) ligands suggest that the latter may be used in conjunction with dopamine D2 antagonists to measure changes in striatal cholinergic function. In this study, the effects of aging on vesicular acetylcholine storage/release were investigated with the high-affinity VR ligand (+)-*meta*-[^{125}I]iodobenzyltrozamicol [(+)-[^{125}I]MIBT]. **Methods:** Male Fischer 344 rats (aged 3 and 24 mo) were injected either with a vehicle or a D2 antagonist [haloperidol or S-(−)-eticlopride]. At prescribed intervals thereafter, all animals were intravenously injected with 10 μCi of (+)-[^{125}I]MIBT. Three hours after radiotracer injection, the animals were killed and their brains dissected. The concentration of radiotracer in the striatum, cortex and cerebellum were then determined. **Results:** In control animals, comparable levels of (+)-[^{125}I]MIBT were observed in corresponding brain regions of young adult and aged Fischer 344 rats. Moreover, in haloperidol- and S-(−)-eticlopride-treated young adult rats, striatal levels of (+)-[^{125}I]MIBT were elevated by 35% and 66%, respectively, relative to controls. In contrast, haloperidol treatment failed to alter the striatal levels of (+)-[^{125}I]MIBT in aged rats while S-(−)-eticlopride displayed a two-fold reduction in potency in aged rats. **Conclusion:** Aging is associated with a reduction in striatal cholinergic plasticity or *striatal cholinergic reserve* and that the D2-stimulated increase in VR ligand binding is a functionally relevant parameter.

Key Words: iodine-125-MIBT vesamicol receptor; cholinergic function; aging

J Nucl Med 1996; 37:1192–1197

The cholinergic system has been implicated in memory and central motor functions (*1–3*). In age-related neurologic disorders, such as Alzheimer's disease, a progressive neurodegenerative disorder associated with: loss of cognitive function and changes in personality, marked reductions in the presynaptic cholinergic markers choline acetyltransferase (ChAT), acetyl cholinesterase (AChE) and sodium dependent high-affinity choline transport (SDHAChT) have been observed in several specific regions of the brain (*4–7*). Although qualitatively similar alterations in cognitive and motor function are associated with normal aging and age-related neuropathology, investigations into the neurochemistry of normal aging have largely yielded conflicting results.

With normal aging, alterations in presynaptic cholinergic markers are either absent or of a much lower magnitude than in age-related neuropathology (*3,8,9*). In spite of these growing body of evidence suggests that the dynamic aspects of central cholinergic neurotransmission are impaired in aging (*10*). Specifically, studies of SDHAChT (an indicator of ongoing neuronal activity and structural integrity) and vesicular acetylcholine ACh (*1*) release in rodents have consistently revealed significant age-related reductions (*10–13*). In the present study, we attempt to assess the effects of aging on ACh storage/release mechanisms with the aid of the radiolabeled vesamicol receptor (VR) ligand (+)-meta-[^{125}I]iodobenzyltrozamicol ((+)-[^{125}I]MIBT) (*14*).

The vesamicol receptor, a unique site on the cholinergic synaptic vesicle, is functionally linked to the vesicular acetylcholine (ACh) transporter (*15*). The prototypical ligand for the VR, (−)-2-(4-phenylpiperidinyl)cyclohexanol (AH5183, vesamicol; Fig. 1), is a potent noncompetitive inhibitor of ACh storage (*16*). Binding of vesamicol to the VR results in the blockade of cholinergic neurotransmission, attributable to the inhibition of both vesicular ACh storage and the subsequent quantal release of ACh. ACh synthesis is, however, unaffected. The location of this receptor presents opportunities for studying the mechanisms underlying the storage and release of ACh. As part of our ongoing effort to validate the use of radiolabeled VR ligands in the study of presynaptic cholinergic function, we demonstrate in this article, with the aid of the VR ligand (+)-[^{125}I]MIBT, that aging is accompanied by a diminution of striatal cholinergic function.

MATERIALS AND METHODS

The radiotracers (+)- and (−)-[^{125}I]MIBT were synthesized as described (*14*) at a specific activity of 1500 ± 200 Ci/mmole.

Received Jun. 2, 1995; revision accepted Oct. 18, 1995.
For correspondence or reprints contact: S.M.N. Efange, PhD, University of Minnesota Hospital and Clinic, Department of Radiology, Mayo Box 292, 420 Delaware St. S.E., Minneapolis, MN 55455.

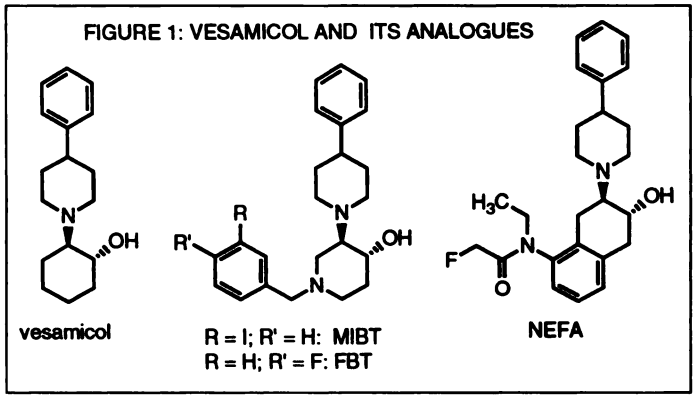

FIGURE 1. Vesamicol and analogs.

Haloperidol, spiperone and S-(−)-eticlopride were obtained for the study as well. Iodine-125-labeled external standards (microscales) for autoradiography were also used. Young adult (age: 3 mo; mean weight, 284 g) and senescent (age: 23 mo; mean weight, 427 g) Fischer 344 rats and Wistar rats were studied (325–370 g).

General Procedure

For each experiment, rats were divided into control and drug-treated groups. At designated times, animals in the control group(s) received either an intraperitoneal injection of the vehicle followed by an intravenous injection of the radiotracer (9–11 μCi) in 100 μl 50% aq. EtOH or a single intravenous injection containing the vehicle and radiotracer. In contrast, animals in the drug-treated group(s) received either an injection of the pharmacologic agent (spiperone or eticlopride) followed by a similar intravenous dose of the radiotracer or a single intravenous injection containing the pharmacologic agent (haloperidol) and the radiotracer. (Since previous unpublished studies had shown that the effects of haloperidol are unaffected by the method of administration, no significant errors should arise from the use of the two injection techniques.) At 5 min or 3 hr following the injection of the radiotracer, the animals were killed by decapitation while under ether anesthesia. The brains were quickly removed, chilled with cold isotonic saline and dissected following the method of Glowinski and Iversen (*17*). The tissues were transferred to pre-weighed sample tubes and subsequently counted in a Beckman gamma scintillation counter. Pre-weighed tubes containing 1-ml samples of a 1:100 dilution of the injected dose were used to determine the cpm for the actual injected dose. For experiments involving both young adult and aged animals, the measured injected dose was converted to a normalized injected dose, prior to calculating the fractional tissue accumulation, to account for the large differences in weights between the age groups. The normalized injected dose = injected dose (cpm) × 1000 g/weight of animal (g). Statistical analysis (ANOVA and Scheffe F-test) was performed with StatView 4.0.

For experiments involving autoradiographic visualization, the following modifications were employed: (1) the dose of radiotracer was increased to 400–500 μCi; and (2) the brains were embedded in Tissue Tek OCT medium, frozen to −38°C and sectioned at −15°C (at a thickness of 20 μ) with a Reichert HistoSTAT cryostat microtome. The sections were later apposed to Kodak NMC film accompanied by external standards. Following exposure and development of the film, the sections were finally subjected to Nissl staining to delineate the cytoarchitecture.

RESULTS

The effects of spiperone, S-(−)-eticlopride and haloperidol on (+)-[^{125}I]MIBT accumulation are presented below. The selection of doses for these compounds was based on a review of the literature on the effects of D2 antagonists on ACh turnover and release (*18–21*).

Effects of Spiperone and S-(−)-Eticlopride on (+)- and (−)-[^{125}I]MIBT Accumulation in Young Adult Wistar Rats

At 3 hr postinjection, the distribution of (+)-[^{125}I]MIBT was high in the striatum, moderate in the cortex and low in the cerebellum, providing striatum:cortex and striatum:cerebellum ratios of 1.93 and 3.42, respectively (Table 1) (*14*). Pretreatment of animals with spiperone (2 mg/kg, intraperitoneal) resulted in increased accumulation of (+)-[^{125}I]MIBT in the striatum. Radiotracer levels in this structure were elevated by 83% ($p = 0.0078$) while those in the cortex and cerebellum either showed a trend toward an increase or were unaffected. Similarly, S-(−)-eticlopride (2 mg/kg, intraperitoneal), a potent and selective dopamine D2 antagonist of the benzamide class, selectively increased the striatal levels of (+)-[^{125}I]MIBT by 66% ($p < 0.0001$) without affecting the radiotracer levels in the cortex and cerebellum.

Consistent with previous reports, the baseline distribution of the less active enantiomer (−)-[^{125}I]MIBT showed little or no regional disparity (Table 2). Following treatment with spiperone, (−)-[^{125}I]MIBT accumulation was increased by 28%–32% ($p < 0.0005$) throughout the brain. In contrast, S-(−)eticlopride

TABLE 1
Effect of Spiperone and S-(−)-eticlopride on the Accumulation of (+)-[^{125}I]MIBT in the Wistar Rat Brain

	%ID/g tissue (±s.e.m.)			
	Control (n = 4)	Spiperone (n = 4)	Control (n = 6)	Eticlopride (n = 6)
Tissue				
Striatum	0.54 ± 0.03	0.99 ± 0.07†	0.59 ± 0.03	0.98 ± 0.03‡
Cortex	0.34 ± 0.03	0.41 ± 0.07	0.30 ± 0.02	0.31 ± 0.01
Cerebellum	0.19 ± 0.02	0.23 ± 0.02	0.17 ± 0.01	0.19 ± 0.001
Striatum-to-Cortex	1.59	2.39	1.93	3.12
Striatum-to-Cerebellum	2.90	4.21	3.42	5.01
	%Dose/Organ			
Whole brain	0.32 ± 0.03	0.42 ± 0.02	0.29 ± 0.02	0.33 ± 0.001

*Spiperone (2 mg/kg) and S-(−)-eticlopride (2 mg/kg) were injected intraperitoneally 15 min prior to radiotracer administration while control animals were injected with the vehicle. All animals were killed 3 hr following radiotracer administration.
†$p = 0.008$; ‡$p < 0.0005$.

TABLE 2
Effect of Spiperone and S-(−)-eticlopride on Accumulation of (−)-[^{125}I]MIBT in Wistar Rat Brain*

	%ID/g tissue (±s.e.m.)		
	Control (n = 4)	Spiperone (n = 4)	Eticlopride (n = 6)
Tissue			
Striatum	1.15 ± 0.03	1.50 ± 0.03†	1.15 ± 0.03
Cortex	1.25 ± 0.03	1.60 ± 0.04†	1.23 ± 0.05
Cerebellum	0.98 ± 0.03	1.30 ± 0.04†	1.01 ± 0.05
	Ratios		
Striatum-to-Cortex	0.92	0.94	0.93
Striatum-to-Cerebellum	1.18	1.16	1.14
	%Dose/Organ		
Whole brain	1.12 ± 0.04	1.48 ± 0.04	1.13 ± 0.05

*Spiperone (2 mg/kg) and S-(−)-eticlopride (2 mg/kg) were injected intraperitoneally 15 min prior to radiotracer administration while control animals were injected with the vehicle. All animals were killed 3 hr following radiotracer administration.
†Significantly different from control ($p < 0.0005$).

failed to alter the levels of this radiotracer in all brain regions examined.

Effects of Haloperidol and S-(−)-Eticlopride on (+)-[^{125}I]MIBT Accumulation in Senescent Rats

Five minutes after the intravenous injection of (+)-[^{125}I]MIBT into male Fischer 344 rats (data not shown), comparable amounts of the radiotracer were detected in the brains of animals from all four groups (young controls, aged controls, young drug-treated and aged drug-treated). Moreover, haloperidol (0–5 μmole/kg) failed to influence the regional distribution of the radiotracer in both young and aged animals (data not shown). Three hours after the intravenous injection of (+)-[^{125}I]MIBT into Fischer 344 rats (Table 3), similar patterns of radiotracer distribution were observed in both young adult and aged controls. Radiotracer levels were highest in the striatum, moderate in the cortex and low in the cerebellum, resulting in striatum:cortex and striatum:cerebellum ratios of 2.88 and 5.75, respectively. In contrast to the conformity observed in the control animals, a divergent pattern was observed following treatment with haloperidol. Following the co-administration of (+)-[^{125}I]MIBT and haloperidol to young adults, radiotracer levels in the cortex and cerebellum were reduced by 38% ($p = 0.003$) and 50% ($p < 0.0001$), respectively. On the other hand, (+)-[^{125}I]MIBT levels in the striatum were elevated by 35% ($p = 0.02$). The combination of increased striatal levels and decreased cortical and cerebellar concentrations produced a two-fold augmentation of the striatum:cortex and striatum:cerebellum ratios which is clearly visible in Table 3 and Figure 2. In aged animals, however, co-administration of (+)-[^{125}I]MIBT with haloperidol only resulted in reduced tracer levels in the cortex and cerebellum. Radiotracer levels in the striatum were unchanged.

In contrast to haloperidol, changes in the regional concentrations of (+)-[^{125}I]MIBT induced by S-(−)-eticlopride (2 mg/kg, intraperitoneal) were restricted to the striatum (Table 4). Specifically, (+)-[^{125}I]MIBT levels in this structure were elevated by 67% ($p < 0.0001$) in young adults and by 38% ($p < 0.0001$) in the aged animals. The difference between these two groups was found to be statistically significant ($p = 0.003$).

DISCUSSION

In a previous study (*14*), we showed that the distribution of the VR ligand (+)-[^{125}I]MIBT in rat brain in vivo is consistent with cholinergic innervation. In addition, we demonstrated that

TABLE 3
Effect of Haldol on Late Phase (3-Hour) CNS Distribution of (+)-[^{125}I]MIBT in Young Adult and Senescent Male Fischer 344 Rats*

	Percent normalized dose/g tissue (±s.e.m.)†			
Tissue	Young adult controls (n = 9)	Aged controls (n = 8)	Haldol-treated young adults (n = 9)	Haldol-treated aged (n = 9)
Striatum	0.23 ± 0.01	0.22 ± 0.004	0.31 ± 0.003‡	0.22 ± 0.01
Cortex	0.08 ± 0.001	0.09 ± 0.003	0.05 ± 0.002‡	0.05 ± 0.002‡
Cerebellum	0.04 ± 0.001	0.05 ± 0.001	0.02 ± 0.001‡	0.03 ± 0.001‡
		Ratios		
Striatum-to-Cortex	2.86	2.59	6.03	4.42
Striatum-to-Cerebellum	5.84	4.13	13.73	8.46
		%Dose/Organ		
Whole brain	0.14 ± 0.001	0.12 ± 0.002	0.09 ± 0.002	0.07 ± 0.002

*Young adult (3 mo) and senescent (23 mo) male Fischer 344 rats were injected intravenously with either a solution of the radiotracer (9–11 μCi) in 100 μl of 50% aqueous ethanol or a solution of the radiotracer combined with haloperidol (0.5 μmole/kg) in the same solvent. Animals were killed at 180 min postinjection.
†The normalized injected dose (see Materials and Methods) takes into account the large differences in weights between the young adult and aged animals.
‡Significantly different from control ($p < 0.05$).

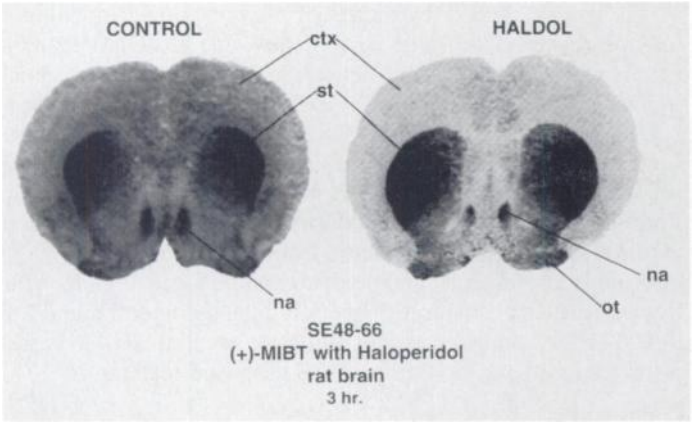

FIGURE 2. Autoradiogram shows distribution of (+)-[^{125}I]MIBT in the rat brain. (Left) Control animal (injected with the radiotracer alone). (Right) Effect of co-administration of tracer with haloperidol. Note the higher striatum-to-cortex and striatum-to-cerebellum ratios resulting from haloperidol treatment.

haloperidol increases the accumulation of this tracer in rat striatum by up to 32% while reducing the radiotracer levels in the cortex and cerebellum. We also showed in a subsequent study (*22*) that the striatal levels of the positron-emitting VR ligand (+)-[^{18}F]FBT were increased by 155% following treatment with haloperidol. Since MIBT displays moderate affinity for σ sites in rat brain tissue (*23*), the haloperidol-induced reductions in (+)-[^{125}I]MIBT binding in the cortex and cerebellum, two regions which are rich in σ sites, were attributed to competition for these binding sites. No satisfactory explanation, however, could be provided for the paradoxical increase in striatal tracer levels. Subsequently, other investigators working with the VR ligand [^{18}F]NEFA (*24*) in the monkey demonstrated, with the use of selective σ and D2 ligands, that the effect of haloperidol (a high-affinity ligand for both dopamine D2 and σ binding sites) in the striatum is mediated by the blockade of dopamine D2 receptors. Dopamine inhibits striatal ACh release via D2 receptors. Accordingly, the blockade of these receptors results in increased release of striatal ACh (*25,26*). On the basis of these functional relationships, Ingvar et al. (*24*) concluded that the binding of VR ligands in vivo reflects the dynamics of cholinergic function.

Since dynamically regulated presynaptic cholinergic processes such as SDHAChT (*10*) and ACh release (*11–13*) have shown a decline in aging we postulated that evaluation of (+)-[^{125}I]MIBT binding in aged animals would constitute an important step in establishing the use of VR ligands for the study of presynaptic cholinergic phenomena. Additionally, the VR is located on cholinergic synaptic vesicles (which account for the majority of ACh released into the synapse). To investigate (and subsequently minimize) the role of confounding factors such as σ binding and perfusion-related phenomena, blockade of dopamine D2 receptors was carried out with haloperidol (a D2 antagonist and potent σ ligand) and the more selective D2 antagonists spiperone and S-(−)-eticlopride. In addition, the effects of these agents on the regional distribution of (−)-[^{125}I]MIBT, the less active enantiomer, were also studied.

At equimolar doses (5.1–5.3 μmole/kg), both spiperone and S-(−)-eticlopride were equally effective at increasing the accumulation of (+)-[^{125}I]MIBT in the striata of young adult Wistar rats (Table 1). Although haloperidol precipitated a smaller response in the striatum (Table 3, (*14*)), a direct comparison with the other D2 antagonists is not possible due to differences in the doses and routes of administration. The generality of the phenomenon is nevertheless supported by the fact that the D2 antagonists haloperidol, spiperone and S-(−)-eticlopride belong to different structural classes. Consistent with the higher selectivity of spiperone and S-(−)-eticlopride for D2 receptors, the levels of (+)-[^{125}I]MIBT in the cortex and cerebellum were unaffected by these agents. Consequently, both spiperone and S-(−)-eticlopride are superior to haloperidol in this paradigm. In contrast to their selective effects on the accumulation of (+)-[^{125}I]MIBT, spiperone and S-(−)-eticlopride displayed disparate effects on the accumulation of (−)-[^{125}I]MIBT. While spiperone was found to induce a global increase in the accumulation of (−)-[^{125}I]MIBT, suggesting enhancement of cerebral perfusion, S-(−)-eticlopride was without effect on the accumulation of this radiotracer. Our observations with S-(−)-eticlopride are consistent with the minimal influence of this agent on cerebral blood flow (*27*). Since the perfusion-enhancing effects of spiperone are nonspecific, we conclude, given their selective effects on the accumulation of (+)-[^{125}I]MIBT, that both spiperone and S-(−)-eticlopride are equally useful in

TABLE 4
Effect of S-(−)-eticlopride on Accumulation of (+)-[^{125}I]MIBT in Young Adult (3 mo) and Senescent (23 mo) Male Fischer 344 Rats*

	Percent normalized dose/g of tissue (±s.e.m.)†			
Tissue	Young adult controls (n = 6)	Eticlopride-treated young adults (n = 6)	Aged controls (n = 6)	Eticlopride-treated aged adults (n = 7)
Striatum	0.27 ± 0.01	0.45 ± 0.01‡	0.26 ± 0.01	0.36 ± 0.02‡
Cortex	0.12 ± 0.004	0.11 ± 0.02	0.14 ± 0.002	0.15 ± 0.02
Cerebellum	0.05 ± 0.003	0.05 ± 0.001	0.07 ± 0.001	0.07 ± 0.01
		Ratios		
Striatum-to-Cortex	2.34	3.93	1.91	2.44
Striatum-to-Cerebellum	5.08	8.97	3.81	5.23
		%Dose/Organ		
Whole brain	0.11 ± 0.002	0.11 ± 0.003	0.12 ± 0.002	0.14 ± 0.01

*Animals in the experimental groups (young and old) were injected intraperitoneally with a solution of S-(−)-eticlopride (2 mg/kg) in 100 μl 50% aq. ethanol while the control animals received a similar volume of the vehicle. After 15 min, (+)-[^{125}I]MIBT was injected intravenously. The animals were killed 3 hr after radiotracer injection.

†The normalized dose takes into account the large differences in weights between the young adult and aged animals.

‡Significantly different from control ($p < 0.05$).

studying the effects of dopamine D2 receptor blockade on striatal cholinergic function.

As reported previously for the Wistar rat (*14*), the early phase distribution of (+)-[^{125}I]MIBT in the Fischer 344 rat was dominated by tracer delivery and was insensitive to haloperidol. Similarly, both haloperidol and S-(−)-eticlopride were found to significantly increase the striatal levels of this radiotracer in young adult Fischer 344 rats at 3 hr postinjection. The similarity between the two rat strains suggests that the D2 effect is not strain specific. In aged Fischer 344 rats, both haloperidol and S-(−)-eticlopride showed significantly diminished potency on the striatal accumulation of (+)-[^{125}I]MIBT, suggesting age-related cholinergic dysfunction. Although the mechanism underlying this reduction is unknown, previous studies (*11–13*) have reported an age-related decrease of comparable magnitude in the evoked release of striatal (and cortical) ACh in Wistar rats in vivo and in rat striatal preparations in vitro. Since vesamicol (and its analogs) bind preferentially to recycling cholinergic synaptic vesicles (*28,29*) which are responsible for the quantal release of ACh into the synapse, and since striatal D2 receptor blockade results in enhanced ACh release (providing an equivalent of evoked release), it is not unreasonable to conclude from the above striking parallels that the age-related refractoriness to D2 blockade detected by (+)-[^{125}I]MIBT reflects diminished dopaminergic control of striatal ACh release. In support of this view, we note that in rat striatal slices a similar age-related decline is observed in the modulation of evoked ACh release by apomorphine, a dopamine agonist (*30*). Further support for a strong connection between ACh release and VR ligand binding is provided by the following observations: (a) in rat phrenic nerve-hemidiaphragm preparations, vesamicol-mediated development of neuromuscular block is frequency dependent (*31*) and (b) vesamicol displays stimulation-dependent inhibition of ACh release in rat striatal slices (*32*). Although it may be argued that the apparent diminished D2-mediated control of cholinergic function simply reflects the age-related loss of striatal D2 receptors (*33,34*), we find a similarly attenuated response to spiperone in the 6-hydroxydopamine(6-OHDA)-lesioned rat (*35*), an animal model characterized by increased D2 receptor density. Consequently, we conclude that the apparent refractoriness of cholinergic neurons to D2 blockade is a complex phenomenon related more to coupling between D2 stimulation and ACh storage/release than to striatal D2 receptor density alone. The complexity of the underlying mechanisms is also suggested by the observation of a similar age-related blunting of haloperidol-mediated neurotensin (a neuropeptide which modulates dopaminergic activity)-mRNA production in the rat striatum (*36*).

CONCLUSION

The functional capacity of the cholinergic system is defined by the totality of interactions which modulate cholinergic activity. If one of these modulatory mechanisms becomes defective, the cholinergic system may become less able to respond to challenge and thus manifest a reduction of plasticity or reserve. Since the dopaminergic-cholinergic interaction partly determines striatal cholinergic plasticity, a reduction in stimulation-release coupling such as we have observed would suggest that the cholinergic functional reserve capacity or cholinergic reserve is diminished in aging. Consequently, we conclude that the neuroleptic-induced increase in the striatal accumulation of VR ligands, such as (+)-[^{125}I]MIBT, is a functionally relevant parameter which may be used to assess striatal cholinergic reserve in vivo. While the reliability of this parameter is yet to be determined, we propose that monitoring of cholinergic reserve by means of pharmacologic modulation may be of diagnostic value. Specifically, one could envision the development of a functional activation or neurostress test which utilizes D2 receptor blockade in combination with a radiolabeled VR ligand to assess cholinergic reserve in human neurologic disorders with PET or SPECT. Such pharmacologically induced functional activation is not new to nuclear medicine. For instance, dipyridamole-induced cardiac stress is used in cardiovascular nuclear medicine to mimic the effects of exercise-induced ischemia on the accumulation of ^{201}Tl in heart tissue. Further evaluation of the VR ligand-spiperone and VR ligand-(−)-eticlopride combinations has been initiated in higher primates to assess the utility of the proposed technique.

ACKNOWLEDGMENT

Financial support for this work was provided by the National Institute of Neurological Disorders and Stroke under grant 1R01NS28711 (SMNE).

REFERENCES

1. Drachman DA. Memory and cognitive function in man: does the cholinergic system have a specific role? *Neurology* 1977;27:783–790.
2. Molchan SE, Mellow AM, Lawlor BA, et al. TRH attenuates scopolamine-induced memory impairment in humans. *Psychopharmacology* 1990;100:84–89.
3. Bartus RT, Dean RL, Beer B, Lippa AS. The cholinergic hypothesis of geriatric memory function. *Science* 1982;217:408–417.
4. Perry RH, Blessed G, Perry EK, Tomlinson BE. Histochemical observations on the cholinesterase activities in the brains of elderly normal and demented (Alzheimer-type) patients. *Age Aging* 1980;9:9–16.
5. Perry EK. The cholinergic system in old age and Alzheimer's disease. *Age Aging* 1980;9:1–8.
6. McGeer PL, McGeer EG, Suzuki J, Dolman CE, Nagai T. Aging, Alzheimer's disease and the cholinergic system of the basal forebrain. *Neurology* 1984;34:741–745.
7. Rylett RJ, Ball MJ, Calhoun EH. Evidence for high-affinity choline transport in synaptosomes prepared from hippocampus and neocortex of patients with Alzheimer's disease. *Brain Res* 1984;289:169–175.
8. Gottfries CG. Neurochemical aspects on aging and diseases with cognitive impairment. *J Neuroscience Res* 1990;27:541–547.
9. Muller WE, Stoll L, Schubert T, Gelmann CM. Central cholinergic functioning and aging. *Acta Psychiatr Scand Suppl* 1991;366:34–39.
10. Sherman KA, Friedman E. Pre- and postsynaptic cholinergic dysfunction in aged rodent brain regions: new findings and an interpretative review. *Intl J Dev Neurosci* 1990;8:689–708.
11. Consolo S, Wang J-X, Fiorentini F, Vezzani A, Ladinsky H. In vivo and in vitro studies on the regulation of cholinergic neurotransmission in striatum, hippocampus and cortex of aged rats. *Brain Res* 1986;374:212–218.
12. Meyer EM, Judkins JH. The development of age-related deficits in several presynaptic processes associated with brain [^{3}H]acetylcholine release. *Mech Aging Dev* 1993;72:119–128.
13. Wu CF, Bertorelli R, Sacconi M, Pepeu G, Consolo S. Decrease of brain acetylcholine release in aging freely-moving rats detected by microdialysis. *Neurobiol Aging* 1988;9:357–361.
14. Efange SMN, Michelson RH, Khare AB, Thomas JR. Synthesis and tissue distribution of m-[^{125}I]iodobenzyltrozamicol ([^{125}I]MIBT): potential radioligand for mapping central cholinergic innervation. *J Med Chem* 1993;36:1754–1760.
15. Parsons SM, Prior C, Marshall IG. Acetylcholine transport, storage and release. *Intl Rev Neurobiol* 1993;35:279–390.
16. Rogers GA, Kornreich WD, Hand K, Parsons SM. Kinetic and equilibrium characterization of vesamicol receptor-ligand complexes with picomolar dissociation constants. *Mol Pharmacol* 1993;44:633–641.
17. Glowinski J, Iversen LL. Regional studies of catecholamines in the rat brain. I. The disposition of [^{3}H]norepinephrine, [^{3}H]dopamine and [^{3}H]Dopa in various regions of the brain. *J Neurochem* 1966;13:655–669.
18. Day J, Fibiger HC. Dopaminergic regulation of cortical acetylcholine release. *Synapse* 1992;12:281–286.
19. Casamenti F, Bianchi C, Beani L, Pepeu G. Effect of haloperidol and pimozide on acetylcholine output from the cerebral cortex in rats and guinea pigs. *Eur J Pharmacol* 1980;65:279–284.
20. Consolo S, Girotti P, Zambelli M, Russi G, Benzi M, Bertorelli R. D1 and D2 dopamine receptors and the regulation of striatal acetylcholine release in vivo. *Progr Brain Res* 1993;98:201–207.
21. Bertorelli R, Zambelli M, Di Chiara G, Consolo S. Dopamine depletion preferentially impairs D1 over D2 receptor regulation of striatal in vivo acetylcholine release. *J Neurochem* 1992;59:353–357.
22. Efange SMN, Mach RH, Khare AB, Michelson RH, Nowak PA, Evora PH. p-[^{18}F]Fluorobenzyltrozamicol ([^{18}F]FBT): molecular decomposition-reconstitution approach to vesamicol receptor radioligands for positron emission tomography. *Appl Radiat Isot* 1994;45:465–472.
23. Efange SMN, Mach RH, Smith CR, Khare AB, Foulon C, Akella SK, Childers SR, Parsons SM. Vesamicol analogs as sigma ligands: molecular determinants of selectivity at the vesamicol receptor. *Biochem Pharmacol* 1995;49:791–797.

24. Ingvar M, Stone-Elander S, Rogers GA, Johansson B, Eriksson L, Parsons SM, Widen L. Striatal D2/acetylcholine interactions: PET studies of the vesamicol receptor. *Neuroreport* 1993;4:1311–1314.
25. Stoof JC, Drukarch B, de Boer P, Westerink BHC, Groenewegen HJ. Regulation of the activity of striatal cholinergic neurons by dopamine. *Neuroscience* 1992;47:755–770.
26. Consolo SP, Girotti P, Zambelli M, Russi G, Benzi M, Bertorelli R. D1 and D2 dopamine receptors and the regulation of striatal acetylcholine release in vivo. *Progr Neurobiol* 1993;98:201–207.
27. Moerlein SM, Perlmutter JS. Specific binding of 3-N-(2'[^{18}F]fluoroethyl)benperidol to primate cerebral dopaminergic D2 receptors demonstrated, in vivo by PET. *Neurosci Lett* 1992;148:97–100.
28. Jope RS, Johnson GVW. Quinacrine and 2-(4-phenylpiperidino)cyclohexanol (AH5183) inhibit acetylcholine release and synthesis in rat brain slices. *Molec Pharmacol* 1986;29:45–51.
29. Searl T, Prior C, Marshall IG. Acetycholine recycling and release at motor nerve terminals studied using (−)-vesamicol and troxylpyrrolium. *J Physiol* 1991;444:99–116.
30. Thompson JM, Makino CL, Whitaker JR, Joseph JA. Age-related decrease in apomorphine modulation of acetylcholine release from rat striatal slices. *Brain Res* 1984;299:169–173.
31. Marshall IG. Studies on the blocking action of 2-(4-phenylpiperidino)cyclohexanol (AH5183). *Br J Pharmacol* 1970;38:503–516.
32. Ricny J, Collier B. Effect of 2-(4-phenylpiperidino)cyclohexanol on acetylcholine release and subcellular distribution in rat slices. *J Neurochem* 1986;47:1627–1633.
33. Morgan DG, Marcusson JO, Nyberg P, Wester P, Winblad B, Gordon MN, Finch CE. Divergent changes in D1 and D2 dopamine binding sites in human brain during aging. *Neurobiol Aging* 1987;8:195–201.
34. Morelli M, Mennini T, Cagnotto A, Toffano G, Di Chiara G. Quantitative autoradiographical analysis of the age-related modulation of central dopamine D1 and D2 receptors. *Neuroscience* 1990;36:403–410.
35. Efange SMN, Langason RB, Khare AB, Low WC. The vesamicol receptor ligand (+)-meta-[^{125}I]iodobenzyltrozamicol ((+)-[^{125}I]MIBT) reveals blunting of the striatal cholinergic response to dopamine D2 receptor blockade in the 6-hydroxydopamine (6-OHDA)-lesioned rat: possible implications for Parkinson's disease. *Life Sci* 1996; 58:1367–1374.
36. Dobie DJ, Merchant KM, Hamblin MW, Vatassery GT, Dysken MW, Dorsa DM. Blunting of the neurotensin mRNA response to haloperidol in the striatum of aging rats: possible relationship to decline in the dopamine D2 receptor expression. *Brain Res* 1993;616:105–113.

Preparation and Biological Evaluation of Iodine-125-IACFT: A Selective SPECT Agent for Imaging Dopamine Transporter Sites

David R. Elmaleh, Alan J. Fischman, Timothy M. Shoup, Chang Byon, Robert N. Hanson, Anna Y. Liang, Peter C. Meltzer and Bertha K. Madras

Division of Nuclear Medicine, Department of Radiology, Massachusetts General Hospital; Department of Radiology, Harvard Medical School, Department of Chemistry, Northeastern University, Boston, Massachusetts; and Organix Inc., Woburn, Massachusetts

Parkinson's disease is a progressive neurodegenerative disorder that is associated with the loss of nerve terminals from specific brain areas, particularly in the caudate and putamen, which contains the highest concentrations of dopamine transporter sites. Previously, we synthesized and evaluated a series of ^{11}C-labeled 2β-carbomethoxy-3β-aryltropane (WIN 35,428; CFT) derivatives as markers for the dopamine transporter system. These ligands have high affinity and specificity for dopamine transporter sites in vitro and in vivo in laboratory animals. The goal of this study was the preparation and preliminary biological characterization of two new ligands based on the structure of WIN 35,428, the E and Z isomers of N-iodoallyl-2β-carbomethoxy-3β-(4-fluorophenyl)tropane (E and Z IACFT). **Methods:** E and Z IACFT were synthesized and radiolabeled with ^{125}I. The ligands were characterized by in vitro assays of binding to dopamine and serotonin transporters and by autoradiography. **Results:** Iodine-125-IACFT was prepared in >60% radiochemical yield, and >98% radiochemical purity. Specific activity was 1500 Ci/mmole. In vitro, E-IACFT showed higher affinity for dopamine transporter sites than WIN 35,428 (6.6 versus 11 n*M*) and better selectivity than RTI-55. The Z isomer was found to have much lower affinity. One hour after an intravenous injection of ^{125}I IACFT in monkeys, ex vivo autoradiographs of the brain revealed high concentrations of tracer in dopamine rich regions such as the caudate-putamen. The striatum-to-cerebellum, striatum-to-cortex and striatum-to-thalamus ratios were 10.8, 7.2 and 8.3. **Conclusion:** These result suggest that radiolabeled E-IACFT may be a useful radioligand for SPECT imaging of dopamine transporter sites. IACFT could prove to be extremely useful for the noninvasive evaluation of patients with early Parkinson's disease.

J Nucl Med 1996; 37:1197–1202

Received Jul. 7, 1995; accepted Sept. 6, 1995.

For correspondence or reprints contact: David R. Elmaleh, PhD, Division of Nuclear Medicine, Massachusetts General Hospital, 55 Fruit St., Boston, MA 02114.

Cocaine is a stimulant and powerful reinforcer that binds to specific recognition sites associated with monoamine transporters (*1,2*). Its primary mechanism of action is ascribed to its ability to bind potently to the dopamine transporter (*3–5*). In 1973, Clarke et al. reported that replacement of the 3-benzoyloxy group in cocaine with a phenyl moiety increases potency by tenfold (*6*). Since then, many cocaine analogs have been prepared and evaluated. (*7–11*) The results of these studies have led to a better understanding of the structure-activity relationship between cocaine analogs and the DA transporter site, however, many questions still remain unanswered.

The cocaine analog, 2β-carbomethoxy-3β-(4-fluorophenyl)-tropane (WIN 35,428; CFT) (Fig. 1:1a), (*6*) has proven to be an important probe for studying these cocaine binding sites in the striatum (*12–18*). Initial studies have revealed that the binding sites for ^{3}H-WIN 35,428 are identical to those of cocaine which are associated with the dopamine (DA) transporter (*19–22*). Tritiated WIN 35,428 binding has been shown to be decreased in postmortem striatal tissue of patients with Parkinson's disease, with a strong correlation between ligand binding and dopaminergic neuron density (*23*). Using a primate model of Parkinson's disease, we demonstrated that when WIN 35,428 is labeled with ^{11}C, disease progression can be monitored noninvasively in vivo by PET (*13*). Recently, these findings were validated in human subjects (*14*).

Although PET with ^{11}C-WIN 35,428 is a useful method for the noninvasive quantification of the density of dopamine terminals, the expense and complexity of this technique limits general applicability. Clearly, a ligand suitable for SPECT would be of significant clinical value. Recently, 2β-carbomethoxy-3β-(4-iodophenyl)tropane (RTI-55, Fig. 1:1b) was synthesized and radiolabeled with ^{125}I (*23*). This compound has